ORIGINAL PAPER

A Study of Vibration Velocity Attenuation Induced by Pneumatic Rock Breaking with Carbon Dioxide Ice Powder for Safety Assessment

Baolin Li[1,2,3,4] · Enyuan Wang[1,2,3,4] · Shaobin Hu[5,6] · Xiaofei Wang[1,2,3,4] · Bing Liu[1,2,3,4]

Abstract

Rock breaking technique plays an important role in rock excavation engineering, such as mining, tunnel construction and hydropower engineering. Pneumatic fracturing with carbon dioxide (CO_2) ice powder is potentially a safe and efficient rock breaking method, which is one of the most pertinent research topics in rock breaking. A site test of pneumatic rock breaking with CO_2 ice powder was carried out on a tuff hill with a compressive strength of 80 MPa. The attenuation of peak particle velocity (PPV) induced by pneumatic rock breaking with CO_2 ice powder was studied and the vibration effect on surrounding buildings was evaluated. The research results demonstrate that: (1) the pneumatic rock breaking with CO_2 ice powder is greatly affected by quasi-static pressure of high-pressure gas with many macrocracks formed near boreholes; (2) with increase in distance, the PPV decreases in the form of a power function with dominant frequency less than 100 Hz, And when the charge of CO_2 ice powder is 4 kg, the PPV reduced down to 21.9 mm/s at the distance of 2.8 m; (3) a simplified motion model of vibration waves propagating in slope is established, showing that the steeper the slope, the faster does the PPV attenuate; and (4) pneumatic rock breaking with CO_2 ice powder is safer than traditional liquid CO_2 and explosive blasting, and it can significantly improve rock breaking efficiency.

Keywords Pneumatic rock breaking · Carbon dioxide ice powder · Peak particle velocity · Vibration monitoring

1 Introduction

With the rapid and sustainable development of global economy, the demand for development and utilization of underground space has been increasing (Sampath et al. 2019). Mining engineering, tunnel construction, hydropower engineering, etc., all require safe and efficient rock excavation. Explosive blasting is the conventional rock breaking technique used for its advantages of high efficiency and economy (Genet et al. 2009; Feng et al. 2020; Hashemi and Katsabanis 2020; Zhou et al. 2020b). However, owing to high-risk impact of blasting shock waves on surrounding buildings and dust pollution, blasting is being strictly regulated and even discouraged (Global 1995; Zhang et al. 2018; Matidza et al. 2020; Roy et al. 2020; Singh et al. 2020; Zhou et al. 2020a). Therefore, various non-explosive rock breaking techniques are being gradually developed as alternatives. Among them, liquid carbon dioxide (CO_2) rock breaking technique has attracted wide attention in the field of rock excavation due to its advantages of low noise, environmental protection, high efficiency and small vibration effect on surrounding buildings (Chen et al. 2017; Gao et al. 2018a;

✉ Enyuan Wang
weytop@cumt.edu.cn

1 Key Laboratory of Gas and Fire Control for Coal Mines, China University of Mining and Technology, Ministry of Education, Xuzhou 221116, Jiangsu, China

2 National Engineering Research Center for Coal Gas Control, China University of Mining and Technology, Xuzhou 221116, Jiangsu, China

3 State Key Laboratory of Coal Resources and Safe Mining, China University of Mining and Technology, Xuzhou 221116, Jiangsu, China

4 School of Safety Engineering, China University of Mining and Technology, Xuzhou 221116, Jiangsu, China

5 Key Laboratory of Ministry of Education for Geomechanics and Embankment Engineering, HoHai University, Nanjing 210098, Jiangsu, China

6 Tunnel and Underground Engineering Institute, College of Civil and Transportation Engineering, HoHai University, Nanjing 210098, Jiangsu, China

Yang et al. 2020). However, the use of high-pressure containers during transportation, filling, handling or storage of CO_2 poses a considerable safety risk. To overcome the shortcomings of the technique, Hu et al. (2019) and Yan et al. (2019) proposed a new pneumatic rock breaking technique using CO_2 ice powder and CO_2 energy agent (CO_2-EA). This technique is characterized by vaporizing CO_2 ice powder through CO_2-EA deflagration heat, thereby breaking rocks through gas shock waves and quasi-static gas pressure generated by the CO_2 phase change, therefore making it safer than liquid CO_2 rock breaking technique. However, there is no related study on the vibration effect of the rock breaking technique on the surrounding buildings.

Vibration monitoring is the conventional method to study the effect of a certain rock breaking technique on surrounding buildings (Gao et al. 2018b; Huang et al. 2020). The effect range of rock breaking-induced vibration can be obtained through the attenuation curve of peak particle velocity (PPV) with distance and allowable blasting vibration safety threshold (for general buildings, the allowable PPV is less than 25 mm/s in China) (Liu and Huang 2019; Kumar and Mishra 2020). Currently, there is no research on the attenuation curve of vibration velocity induced by pneumatic rock breaking with CO_2 ice powder, but is mainly focused on the field of explosive rock breaking. To get the attenuation curve of PPV with distance, many empirical formulas, as shown in Table 1, were proposed about the vibration induced by explosive blasting (Duvall and Fogelson 1962; Davies et al. 1964; Ambraseys and Hendron 1968; Roy 1991; Monjezi et al. 2013). The main parameters of these formulas refer to blasting charge, blasting distance and geological conditions. Owing to the complex influencing parameters, the empirical formulas may not entirely adapt to all actual situation. With the development of artificial intelligence techniques, more and more artificial intelligence

tools such as artificial neural networks (ANNs), hidden Markov models, fuzzy models and neuro-fuzzy models are being employed for the attenuation of the PPV induced by explosive blasting (Khandelwal and Singh 2007; Jahed et al. 2014, 2015; Radojica et al. 2014; Hajihassani et al. 2015; Bayat et al. 2020). However, there are differences in governing principle between pneumatic rock breaking with CO_2 ice powder and explosive rock breaking. Explosive rock breaking mainly uses high-temperature and high-pressure explosive gas generated by violent chemical reaction. The impact damage to the surrounding rock is serious, forming an obvious crushing zone around the borehole (Donzé et al. 1997). Pneumatic rock breaking with CO_2 ice powder mainly uses the quasi-static action of high-pressure gas produced by the CO_2 ice powder gasification, which is a physical change. Therefore, the empirical formulas for studying the attenuation of PPV induced by explosive blasting may not be applicable to pneumatic rock breaking with CO_2 ice powder. Besides, to study the impact of vibration on surrounding buildings, the vibration frequency is also important as well as PPV. If the vibration frequency induced by rock breaking is close to the natural frequency of buildings, resonance occurs easily, which is a serious threat to the safety of buildings (Khandelwal and Singh 2006; Wang et al. 2015; Roy et al. 2016). It is generally believed that the vibration at the frequency of 5–10 Hz has greater damage potential of structural damages than the high-frequency vibration at a specific velocity (Yang et al. 1994; Nateghi et al. 2020).

This paper carried out on-site rock breaking test using pneumatic rock breaking technique with CO_2 ice powder. To analyze the effect of rock breaking-induced vibration on surrounding buildings, vibration sensors were installed near the rock breaking site and vibration waveforms were acquired in real time by the microseismic monitoring system. The PPV and the dominant frequencies of vibration waveforms at different distances were obtained and their attenuation with distance was analyzed. In addition, waveform characteristics, rocking breaking efficiency and cost were compared between a hydraulic breaker and pneumatic rock breaking with CO_2 ice powder. The study results are important for the future industrial implementation of safer CO_2 rock breaking technique and guidelines.

2 Experimental Test

2.1 Site and System of Rock Breaking

2.1.1 Rock Breaking Site

The rock breaking site, shown in Fig. 1, is located in Hangzhou City, Zhejiang Province, China, where tunnel construction was under way. The tuff hill with compressive strength

Table 1 Different empirical formulas for predicting PPV induced by explosive blasting (Monjezi et al. 2013),

Empirical formulas	Equation
USBM (Duvall and Fogelson 1962)	$PPV = K \times \left[\frac{D}{\sqrt{W}} \right]^n$
Ambraseys–Hendron (1968)	$PPV = K \times \left[\frac{D}{W^{0.33}} \right]^n$
Davies et al. (1964)	$PPV = \frac{K \times D^b}{W^{-a}}$
Indian Standard (1973)	$PPV = K \times \left[\frac{W}{D^{2/3}} \right]^{-n}$
Roy (1991)	$PPV = a + K \times \left[\frac{D}{\sqrt{W}} \right]^{-n}$

PPV means peak particle velocity (mm/s), D is the distance from the explosive position (m), W is the maximum explosive charge per delay (kg) and K, a, b and n are the site constants, which can be calculated by multiple regression analysis
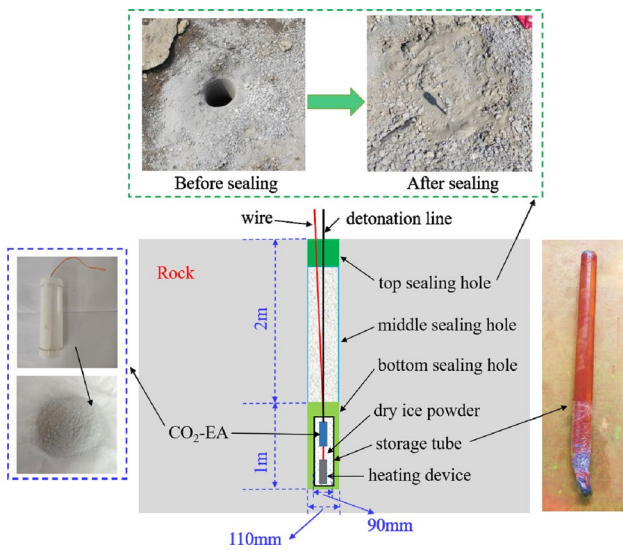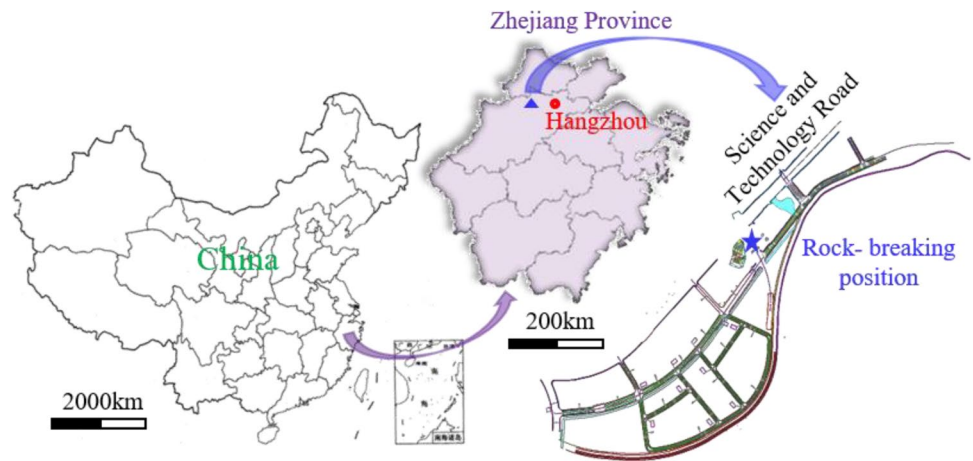
Fig. 1 Rock breaking site

Fig. 2 Pneumatic rock breaking system with CO_2 ice powder

of 80 MPa needed to be demolished in the construction area. As the area was close to the subway and residential buildings, explosive blasting was prohibited. Mechanical rock breaking using a hydraulic breaker was carried out, but its efficiency was very low. To improve construction efficiency, pneumatic rock breaking tests with CO_2 ice powder were carried out in this area.

2.1.2 Rock Breaking System

The pneumatic rock breaking with CO_2 ice powder system, as shown in Fig. 2, is mainly composed of CO_2 ice powder, CO_2-EA, heating device and a storage tube with a diameter of 90 mm and a length of 1000 mm. CO_2-EA is a high-energy material which burns violently in different physical states of CO_2 and releases a lot of heat under specific temperature and pressure conditions. In contrast, it

has stable properties in the air. Before the test, CO_2-EA had been pressed into PVC tubes. Two boreholes were used to break rock with a diameter of 110 mm and a depth of 3 m. After putting the storage tube into a borehole, the remaining length of the borehole to be sealed was 2 m. CO_2 ice powder in each storage tube weighed 4 kg. Under high-voltage excitation, the CO_2-EA burned violently and released heat, causing rapid gasification of CO_2 ice powder and resulting in fracturing the rock.

2.2 Microseismic Monitoring System and Monitoring Network Layout

To determine the attenuation law of PPV with the increasing distance and the effect range of the induced vibration, the process of rock breaking was monitored by a KJ522 microseismic (MS) monitoring system. It mainly consists of KJ522-F mine-used intrinsically safe MS monitoring substation, GZD3 vibration sensors and monitoring server, computer server and junction boxes. The KJ522-F monitoring substation has 16 channels, and the AD conversion precision of each channel is 24 bits. The input range for each channel could be ± 10 V, ± 5 V, ± 2.5 V, 0–10 V and 0–5 V, and the used one in this test was ± 10 V. The highest sampling frequency for each channel could be up to 250 kHz, and it was set at 2 kHz for each channel in the test. The GZD3 vibration sensors have a frequency response range 0.1–500 Hz. The MS monitoring system acquired data based on a defined triggering method. Only when the amplitude of waveform acquired by any one channel was higher than the trigger amplitude (0.05 mm/s set in the test), the waveforms of all channels were recorded, and the time window length was set to 512 ms for each channel to record data. The vibration sensors arrangement network and the top view of rock breaking position, as shown in Fig. 3, contain 13 vibration sensors. S14 and S13 were arranged on the rock near the rock breaking position, and other vibration sensors were all
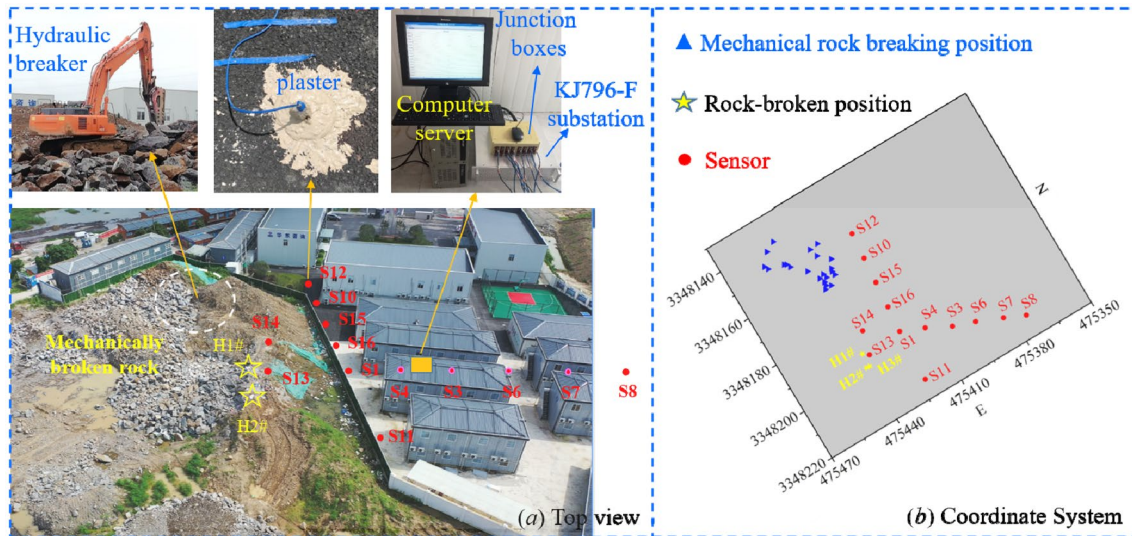
Fig. 3 MS monitoring system and monitoring network layout

arranged near the accommodation buildings of the project. It was mainly arranged along two survey lines to study the effect of pneumatic rock breaking with CO_2 ice powder on the stability of surrounding buildings. The distances between S1, S4, S3, S6, S7 and S8 sensors and between S1, S16, S15, S10 and S12 sensors were all 10 m. To fully couple the sensors with the ground, they were fixed with a mixture of gypsum powder and water, and the test was performed after the plaster hardened. To prevent the wires' jitter from interfering with the monitoring, the wires were fixed with tape.

3 Vibration Attenuation Induced by the Hydraulic Breaker

Before performing pneumatic rock breaking test using CO_2 ice powder, a hydraulic breaker was working near the test site (as shown in Fig. 3). It was designed with hammer body weight 2986 kg, operating weight 3950 kg, impact frequency 230–320 bpm/min, operating pressure 19–21 MPa, impact energy 11,455 J and output power 52 kW. To compare the vibration induced by pneumatic rock breaking with CO_2 ice powder, the vibration induced by the hydraulic breaker was monitored for a long time.

3.1 Vibration Waveforms Induced by the Hydraulic Breaker

Figure 4 shows all vibration waveforms induced by an impact of the hydraulic breaker. The waveforms from top to bottom in the figure are recorded by sensors with increasing distance from the rock breaking site. The closer the sensor to the rock breaking locale, the higher is the PPV, and
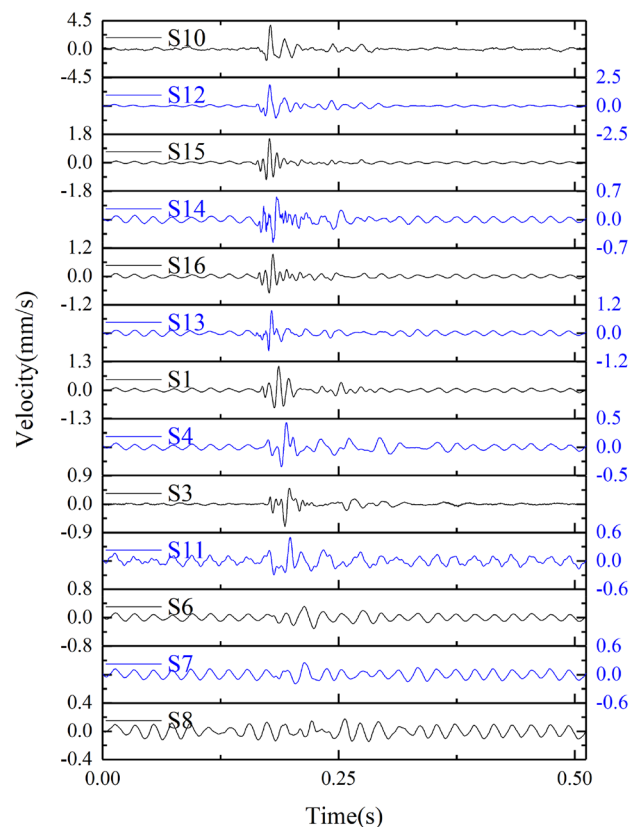

Fig. 4 Waveforms induced by the mechanical rock breaking

the more obvious is the first arrival time and end time of the waveforms. On the whole, the waveforms take off (the rising process from the first arrival time to the peak) and attenuate after peak rapidly, lasting for a short time of about
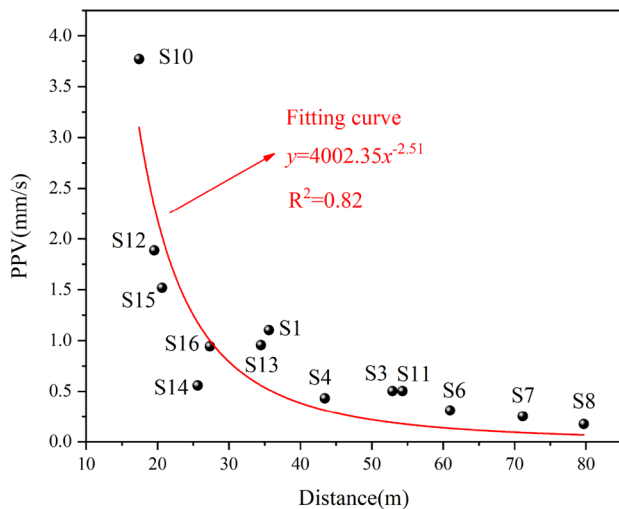
Fig. 5 Attenuation of the PPV with distance

70 ms. The attenuation of the PPV of each waveform with the distance from the rock breaking location is shown in Fig. 5. With the increase of distance, the PPV decreases on the whole. The PPV recorded by the sensor S10 that is closest (17.4 m) to the rock breaking site is 3.78 mm/s, which is much smaller than the threshold (25 mm/s) for vibration velocity of general buildings in the safety standard of blasting vibration. Gao et al. (2007) found that shock and vibration energy in rock and soil media attenuates exponentially with the propagation distance. Therefore, scatter plots of the relationship between the PPV and the distance were fitted by a power function ($y = ax^{-b}$), thus obtaining a fitting accuracy R^2 (coefficient of determination) 0.82. It can be considered that the attenuation of the PPV induced by the hydraulic breaker basically conforms to the power function, and the index b obtained by fitting can evaluate the attenuation degree of the vibration velocity, which is known as an attenuation coefficient. The larger the b, the faster does the vibration velocity attenuate with increasing distance.

To study the impact of vibration on surrounding buildings, the vibration frequency is also important as well as PPV. Fourier transform, as one of the most classical and widely used frequency analysis methods, is generally suitable for studying overall distribution of waveform frequency. The calculation formula is shown as follows (Xu et al. 2010; Li et al. 2017a, b):

$$F(w) = \int_{-\infty}^{\infty} f(t)e^{-jwt}dt \qquad (1)$$

where, t, w and j represent the time, frequency and the imaginary unit which is equal to the square root of -1, respectively; e indicates the base of natural logarithms. For the signal processing in this study, the MATLAB command

fast Fourier transform (FFT) was used to perform the frequency spectrum analysis. Frequency spectrums of all waveforms are demonstrated in Fig. 6. The spectrum from top to bottom are sorted out at positions with increasing distance from the rock breaking point (to facilitate comparison, the waveform spectrums are shifted). It can be observed that the main energy of waveforms distributes in the range of 8–168 Hz. With increasing distance, high-frequency components attenuate rapidly. In terms of the complexity of the frequency distribution, apart of the corresponding spectrum of S10, others are relatively simple with distinct dominant frequencies. Overall, the dominant frequencies of waveforms do not change significantly with the increasing distance. The dominant frequencies of two sensors (S10, S12) closest to the rock breaking point are the same (about 60.5 Hz), while those for other sensor waveforms are about 50.8 Hz with a slight reduction. Owing to dominant frequencies of waveforms more than 50 Hz, and the PPV of only 3.78 mm/s at about 17.4 m, the hydraulic breaker will cause less damage to the surrounding buildings.

3.2 Attenuation of the PPV Induced by the Hydraulic Breaker

Fifty MS events induced by the hydraulic breaker were randomly selected from the database of MS minoring system. Based on this, the distances between the source locations of each vibration event and all vibration sensors were calculated and the PPV of all waveforms were calculated. The statistical results of attenuation of the PPV of 50 events with different distances were obtained, as shown in Fig. 7a. The scatter plots of attenuation of the PPV of all events with distance were fitted by the power function. Furthermore, by taking the fitting coefficient b as the attenuation coefficient, the
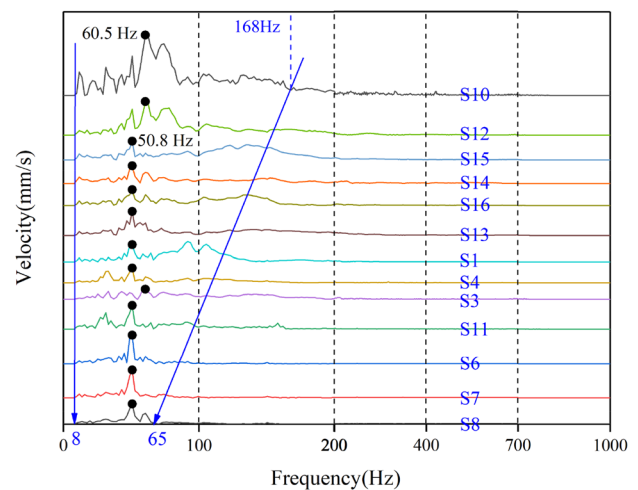

Fig. 6 Waveform spectrums

(a) Scatter plot of the PPV with the distance

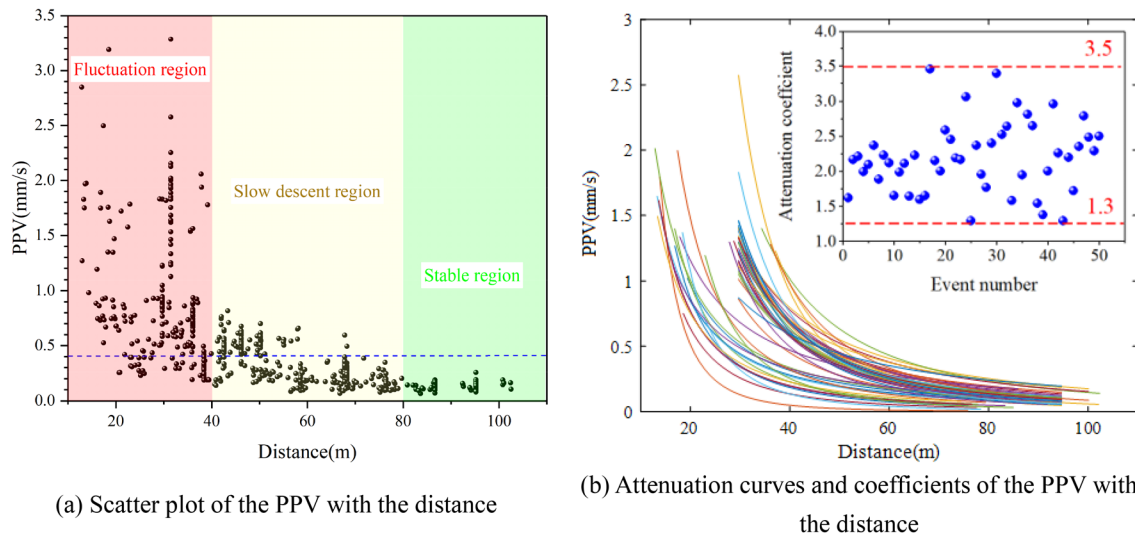(b) Attenuation curves and coefficients of the PPV with the distance

Fig. 7 Attenuation of the PPV induced by mechanical rock breaking with the distance. **a** Scatter plot of the PPV with the distance. **b** Attenuation curves and coefficients of the PPV with the

attenuation curves and coefficients of the vibration velocities of 50 events with the distance were obtained, as displayed in Fig. 7b.

As illustrated in Fig. 7a, the PPV induced by the hydraulic breaker are smaller than 3.5 mm/s beyond the distance of 10 m. This velocity is far smaller than the requirement for vibration velocity threshold (25 mm/s) of general buildings in the allowable safety standards for blasting vibration. Compared with Fig. 7b, it can be seen that the attenuation of the PPV corresponding to different ranges of the distance have differences, which can be basically divided into three stages. To be specific, in rapid descent region within 40 m, the PPV attenuates most rapidly. The maximum PPV is 3.3 mm/s, while the minimum one is only 0.2 mm/s. In slow descent region with the distance within 40–80 m, the maximum PPV of the waveform attenuates slowly with fluctuations in a range of 0.1–1 mm/s. In stable region within 80–100 m, the PPV is largely unchanged and the PPV changes from 0.1 to 0.3 mm/s. Attenuation coefficients of vibration velocities induced by the hydraulic breaker range from 1.3 to 3.5 and are mainly distributed in the range of 1.5–2.5.

4 Vibration Attenuation Induced by Pneumatic Rock Breaking with CO_2 Ice Powder

4.1 Vibration Waveforms Induced by Pneumatic Rock Breaking with CO_2 Ice Powder

CO_2 ice powder was used for the pneumatic rock breaking twice, separately corresponding to boreholes H1 and H2

(rock breaking therein was conducted separately). Figure 8 shows the vibration waveforms induced by two rock breaking events with CO_2 ice powder (the waveforms from top to bottom are obtained at positions with increasing distance from the rock breaking position). With increasing distance, the velocity of the waveform diminishes. The difference in the first arrival time of different waveforms is obvious. The farther away from the source, the later the sensors receive the waveforms, which reflect the vibration propagation from near to far zones. In comparison with the vibration waveforms induced by the hydraulic breaker, the vibration waveforms induced by the pneumatic rock breaking with CO_2 ice powder take off and attenuate slower and the fluctuation lasts longer for about 125 ms.

Performing FFT on all waveforms gave spectrums of all waveforms are shown in Fig. 9. The spectrum distribution of pneumatic rock breaking-induced vibration is more complex than that of the hydraulic breaker. There are numerous low-frequency components below 50 Hz and the dominant frequencies mainly lie between 10 and 50 Hz. In case the vibration velocity in both the scenarios is the same and higher than the allowable limit, the damage of pneumatic rock breaking-induced vibration to surrounding buildings is more intense than that of the hydraulic breaker. The distribution of main energy in spectrum of vibration waveforms induced by the pneumatic rock breaking with CO_2 ice powder gradually converges with the increase in distance. It reveals that the attenuation of high-frequency components with the distance is faster than that of low-frequency components. Therefore, more attention should be paid to the low-frequency components when evaluating the effects of vibration induced by rock breaking on surrounding buildings or infrastructures.
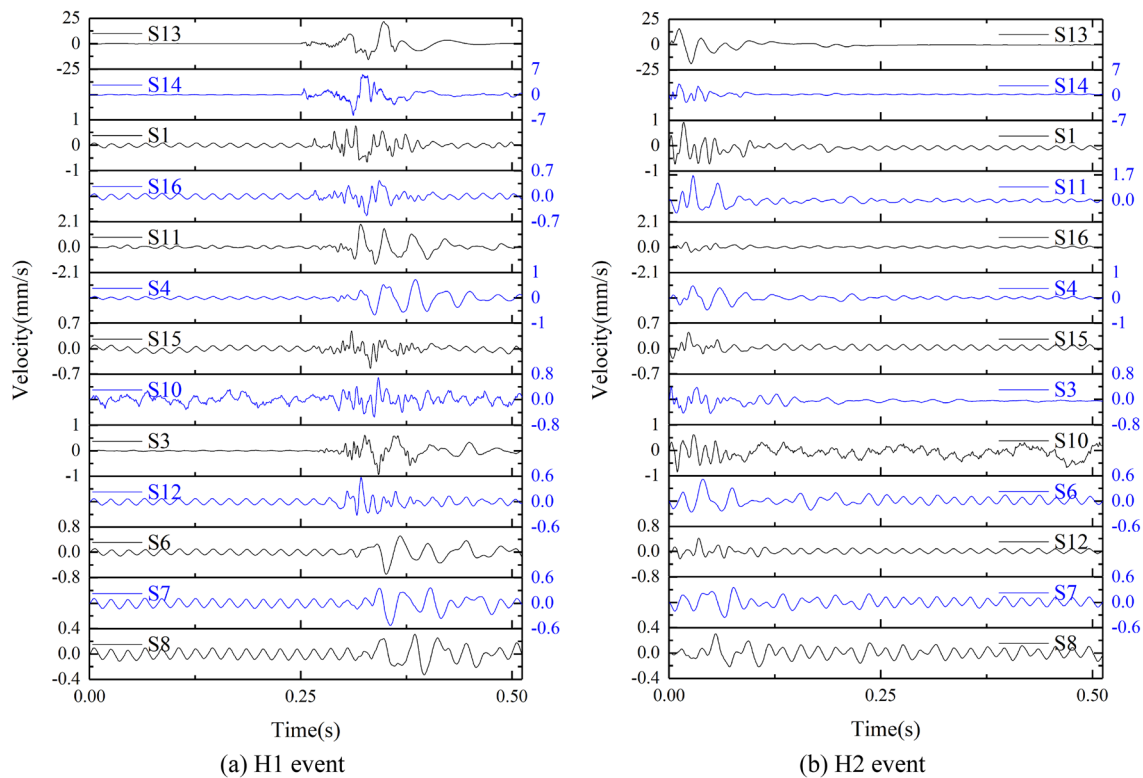
Fig. 8 Vibration waveforms induced by pneumatic rock breaking with CO_2 ice powder. Distance. **a** H1 event. **b** H2 event
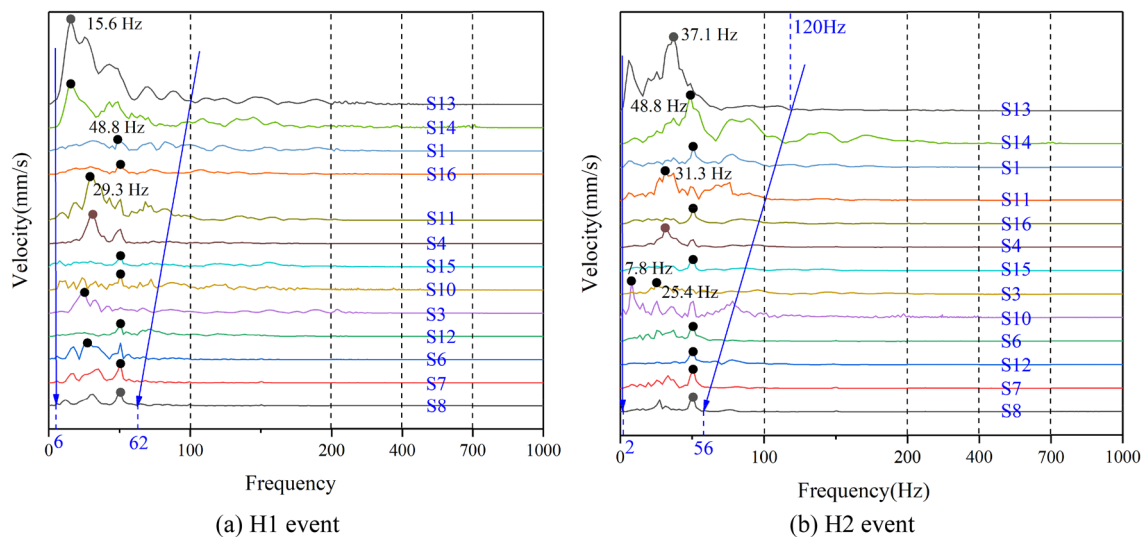

Fig. 9 Spectrums of the vibration waveforms induced by pneumatic rock breaking with CO_2 ice powder. **a** H1 event. **b** H2 event

However, unlike the hydraulic breaker, the dominant frequencies of vibration waveform induced by pneumatic rock breaking vary greatly with the increasing distance. The dominant frequencies of waveforms close to the rock breaking point are generally lower as recorded by S13. However, it is not that the larger the distance, the higher the dominant frequency of the waveform. Both in the waveforms and spectrum distribution, the two farthest sensors (S7, S8, the distance from rock breaking position corresponds to 57.6 m and 66.6 m, respectively) have small differences, indicating that the vibration velocity and frequency attenuate significantly within a certain distance range (below 57 m). More than 57 m

away from the rock breaking point, the vibration velocity and frequency will not change considerably.

4.2 Attenuation of Vibration Velocity Induced by Pneumatic Rock Breaking with CO_2 Ice Powder

The vibration velocity induced by two events of the pneumatic rock breaking with CO_2 ice powder with the distance was obtained, as displayed in Fig. 10. The sensor S13 is closest (2.8 m) to the rock breaking point, and the PPV is 21.9 mm/s, which is smaller than the threshold allowable vibration velocity of general buildings (25 mm/s). Owing to the fact that the PPV attenuates with the distance on the whole, the effect distance of the vibration induced by the pneumatic rock breaking with CO_2 ice powder on the safety of surrounding buildings should be less than 3 m, which is much smaller than the safety distance (5 m) of the traditional rock breaking with liquid CO_2 (Li et al 2018, 2020; Liu and Huang 2019). Compared with attenuation of the vibration velocity induced by the hydraulic breaker, attenuation of the vibration velocity induced by the rock breaking with CO_2 ice powder more closely conforms to the power function and the fitting accuracy is 0.95. Therefore, the power function can be used to predict the vibration velocity within any distance. Similar to the hydraulic breaker, attenuation of the vibration induced by the rock breaking with CO_2 ice powder can also be divided into three regions, that is, rapid descent region (0–16 m), slow descent region (16–50 m) and stable region (50–70 m) of vibration velocity. The difference is that the vibration velocity induced by the pneumatic rock breaking with CO_2 ice powder attenuates slower, as reflected by the attenuation coefficient (1.26) that is smaller than that
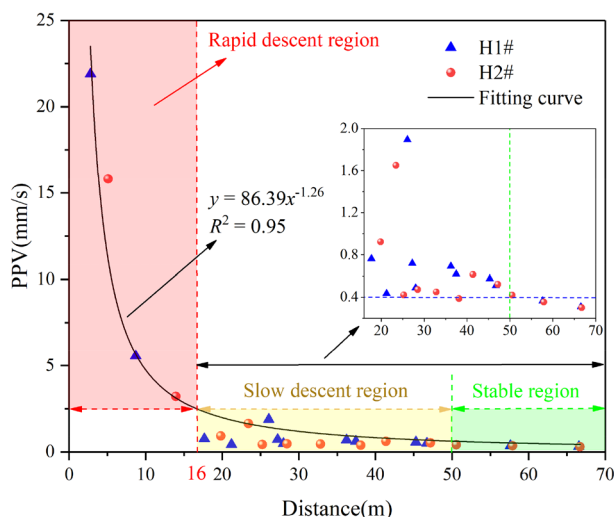

Fig. 10 Attenuation curve of the PPV induced by the pneumatic rock breaking with CO_2 ice powder with the distance

of the vibration velocity induced by the hydraulic breaker. Moreover, the vibration velocity induced by the pneumatic rock breaking with CO_2 ice powder is generally greater than that of the hydraulic breaker when the distance is the same.

5 Discussion

5.1 Comparison of Waveforms Induced by the Hydraulic Breaker, Pneumatic Rock Breaking with CO_2 Ice Powder and Rock Breaking with Explosives

Mechanized rock breaking tools mainly include hydraulic rock splitter, hydraulic breaker and tunnel boring machine (TBM). A hydraulic breaker is mainly used for secondary rock crushing, urban engineering, etc. It mainly causes tensile failure of rock through rapid and strong impacts on rock using the tip of a hardened tool. Owing to the short action time and propagation of the vibration mainly in the shallow ground media, the vibration waveform induced by the hydraulic breaker lasts for a short time, and the vibration velocity attenuates rapidly. This is different from the vibration waveforms caused by TBM, which lasts longer (Carnevale et al. 2000; Grund et al. 2016; Huang et al. 2018). Owing to the small damage area caused by the hydraulic breaker, the fracture form of rock is relatively simple, so the spectrums of hydraulic breaker waveforms are relatively simple with high dominant frequencies (more than 50 Hz). Figure 11 shows the typical waveform and frequency spectrum of the vibration waveform induced by the rock breaking with explosives. It can be observed that velocity attenuates fast after peak, which reflects fast and large energy release from such rock breaking process. In the traditional explosive blasting, most of the energy is consumed as shock waves in the range that is twice the blasting borehole radius from the center of the blasting borehole. In this range, a crushed zone and a broken zone are formed under the dynamic action of stress waves and quasi-static action detonation gas (Chi et al. 2019). Due to the large range of crushed and the broken rock, spectral distribution of the vibration waveforms induced by explosives blasting is more complex than that of pneumatic rock breaking with CO_2 ice powder and the hydraulic breaker. The frequency distribution range of main energy is considerably wide (0–225 Hz) with dominant frequency at about 25 Hz. The process of pneumatic rock breaking with CO_2 ice powder can be divided into two stages. Stress waves are produced first due to impacts of high-pressure CO_2 on the wall of the borehole, so that microcracks are formed around the wall. Then the impact fracture and primary fracture continue to propagate under the quasi-static pressure due to expansion of high-pressure CO_2 gas. The action time for first stage is very short, while long for the second stage. The quasi-static
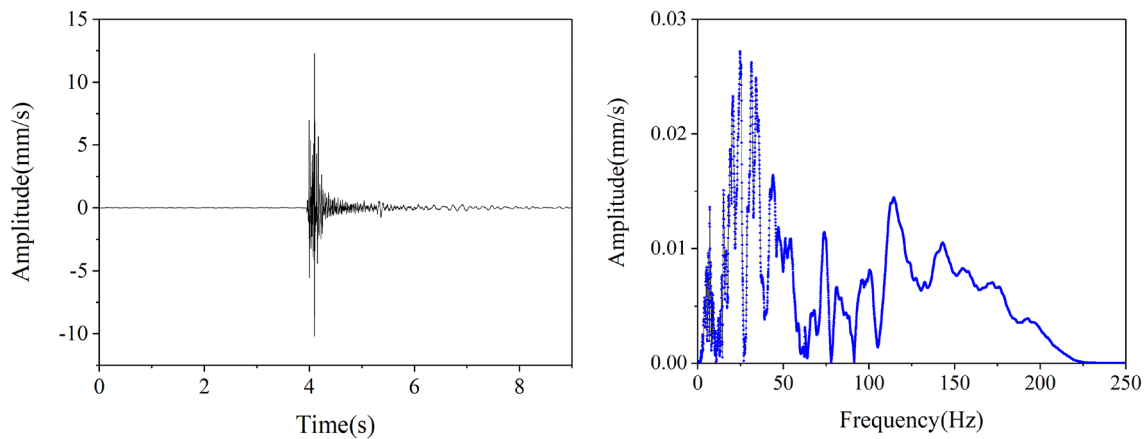
Fig. 11 Waveform and spectrum induced by explosive blasting

pressure of high-pressure CO_2 gas is the main cause of rock breaking. This explains why the vibration waveform induced by the pneumatic fracturing with CO_2 ice powder takes off and attenuates slowly after peak velocity, and the attenuation of the PPV with the distance is weaker than that of the hydraulic breaker. The positions of rock breaking boreholes are relatively stable, and there is no obvious difference before and after rock breaking, as is evident from field pictures taken after the pneumatic rock breaking with CO_2 ice powder (Fig. 12). However, obvious macrocracks are formed around the boreholes, which in contrast to the rock breaking with explosives is quite different, that is, there is no obvious crushing zone around the boreholes, and the main damage pattern is macrocracks around the fracturing boreholes.

5.2 Influences of the Slope on Attenuation of Vibration Induced by Pneumatic Fracturing with CO_2 Ice Powder

According to the rectangular coordinates of sensors and the boreholes H1 and H2, the polar coordinate system is established. In accordance with the PPV recorded by sensors in different positions, the contour map of polar coordinates is drawn, as shown in Fig. 13a and b, which correspond to boreholes H1 and H2, respectively. It can be concluded that attenuation of the PPV in different directions has certain differences. Obviously, it is faster along the direction of the sensor S1 than that along the direction of the sensor S11. Analysis suggests the slope to be the main reason behind this effect. Elevations of the boreholes H1 and H2 are higher than that of the position where the sensors S1 and S11 are located (Fig. 14). The vibration waves induced by the pneumatic rock breaking with CO_2 ice powder are transmitted downward from the rock breaking point to the vibration sensors. They will not be transmitted in a straight line, but repeatedly reflected and refracted on the slope before reaching the sensors. The actual propagation process is

complex. To simplify the analysis, a simplified motion model for vibration wave propagation through the slope was established. Assuming that P-waves propagate from one medium to another as incident waves, they disturb particles in the two media and then are reflected and refracted on the interface. In this case, the distribution of wave impedance on the upper and lower interfaces of rock mass plays a key role in the refraction and reflection of stress waves. Based on the wave theory and law of energy conservation, the relationship between the velocity and stress of particles on the upper and lower interfaces is expressed as follows (Tang 2007; Zhong 2018):

$$\begin{cases} v_T = v_I + v_R \\ \sigma_T = \sigma_I + \sigma_R \\ \dfrac{\sigma_T}{\rho_2 C_2} = \dfrac{\sigma_I}{\rho_1 C_1} - \dfrac{\sigma_R}{\rho_1 C_1} \end{cases} \tag{2}$$

where v and σ indicate the velocity and stress of the particle, respectively; subscripts I, T and R respectively represent the incident, refracted and reflected waves; ρ_1 and ρ_2 denote the densities of the upper and lower media; C_1 and C_2 stand for the wave velocities in the media. The relationship of σ with ρ, C and v is shown as follows:

$$\sigma = \rho C v \tag{3}$$

By combining Formulas (2) and (3), the following formulas are obtained:
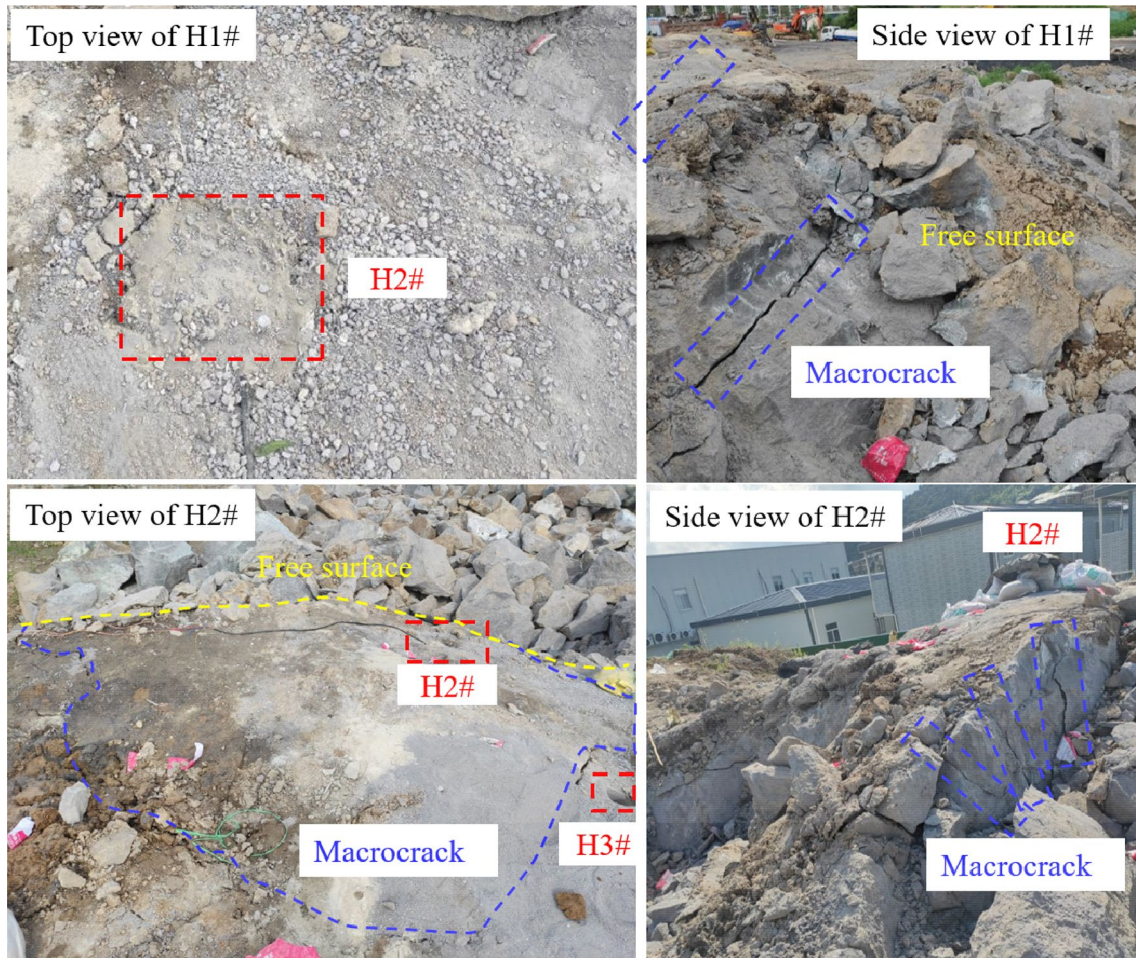
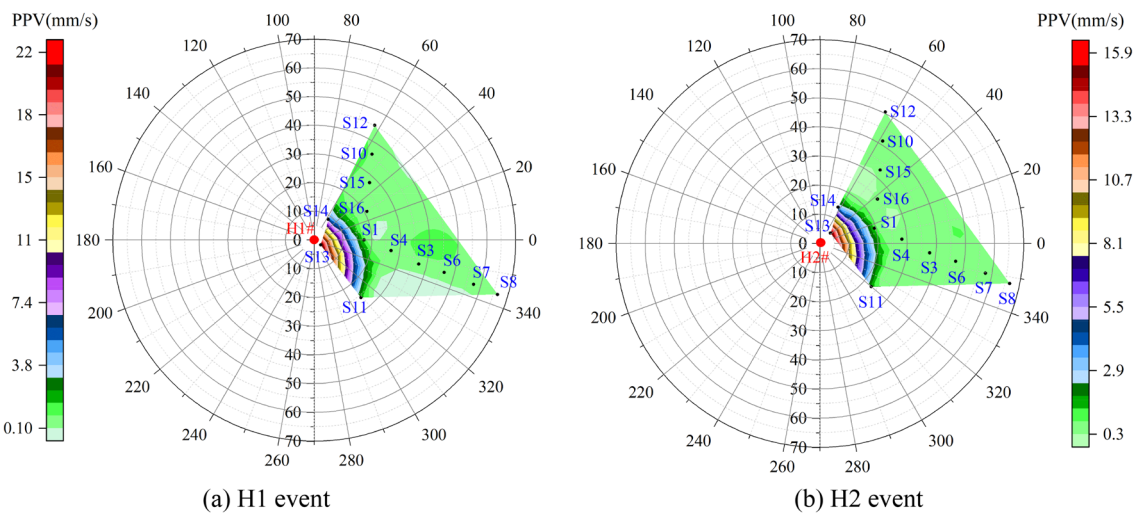**Fig. 12** Photos of rock breaking in the field

Fig. 13 Distribution contour map of the PPV under polar coordinates. **a** H1 event. **b** H2 event
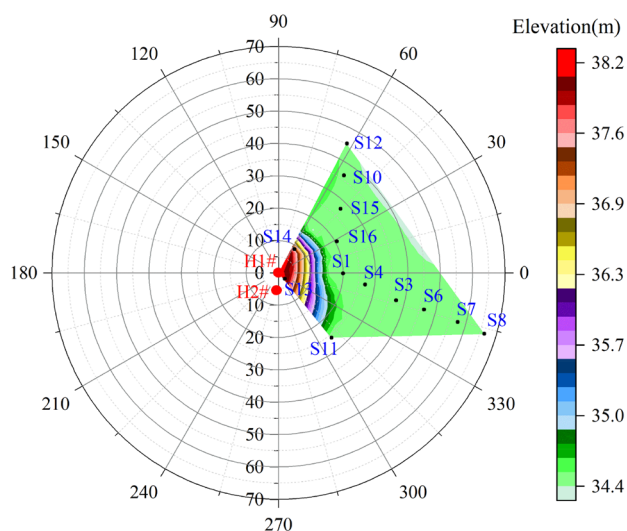
Fig. 14 Contour map of elevation under polar coordinates

$$\begin{cases} \dfrac{\sigma_R}{\sigma_I} = \dfrac{\rho_2 C_2 - \rho_1 C_1}{\rho_2 C_2 + \rho_1 C_1} \\[2mm] \dfrac{\sigma_T}{\sigma_I} = \dfrac{2\rho_2 C_2}{\rho_2 C_2 + \rho_1 C_1} \\[2mm] \dfrac{v_R}{v_I} = \dfrac{\rho_1 C_1 - \rho_2 C_2}{\rho_2 C_2 + \rho_1 C_1} \\[2mm] \dfrac{v_T}{v_I} = \dfrac{2\rho_1 C_1}{\rho_2 C_2 + \rho_1 C_1} \end{cases} \quad (4)$$

Wave impedance on the interface generally increases from the shallow part to the deep part. Therefore, the vibration induced by the pneumatic rock breaking with CO_2 ice powder propagates downward and $\rho_2 C_2$ is larger than $\rho_1 C_1$. Moreover, $\sigma_R > 0$, $v_R < 0$ and $v_T < v_I$. In other words, after the vibration waves propagate downward, the intensity decreases, and the particles move in an opposite direction to the particles of the incident waves. There is a small difference of elevation between the two breaking boreholes and the elevations of the sensors S1 and S11 are the same. However, along the direction toward sensor S1, elevation rapidly decreases and the slope is very steep. Along the direction of the sensor S11, the elevation changes relatively slowly and the slope is gentle. Therefore, it can be considered that the presence of the slope accelerates attenuation of the vibration velocity. The steeper the slope, the more are the absorption and refraction of the vibration waves traveling through the slope to reach the vibration sensors and the greater is the consumption of vibration energy. Therefore, the vibration velocity along the direction of the sensor S1 attenuates more rapidly.

5.3 Comparison of Efficiency and Cost

There are two significant advantages for the technique of pneumatic rock breaking with CO_2 ice powder. One is small vibration effect on surrounding buildings; the other is that the energy for breaking rock comes from the phase change of CO_2, and the main materials used are CO_2 ice powder and non-explosive energy agent. Thereby, the construction is safe and controllable. When it comes to the efficiency and cost, the hydraulic breaker can be for a comparison. The rock breaking efficiency of a hydraulic breaker in the test is about 8 m^3/h. For pneumatic rock breaking with CO_2 ice powder, the rock breaking efficiency is affected by many factors, such as site geological properties (rock strength, geological discontinuities, etc.), drilling speed, number of boreholes and charge of CO_2 ice powder (Li et al. 2020). The efficiency and cost are analyzed based on the field test. Time consumption is mainly concentrated on drilling boreholes and installations of tubes. The drilling velocity is about 0.2 m/min using a hydraulic rock drill in the test and takes about 30 min drilling for two boreholes. The transportations and installations of tubes cost about 60 min. The total volume of broken rock caused by pneumatic rock breaking is 30 m^3. Therefore, the rock breaking efficiency of pneumatic rock breaking with CO_2 ice powder can reach up to 20 m^3/h. Pneumatic rock breaking not only produces large piece of rocks, but also creates free surfaces. It significantly improves the rock breaking efficiency of the hydraulic breaker. Consider all energy consumption and costs, pneumatic rock breaking with CO_2 costs lower than a hydraulic breaker at the same rock breaking volumes.

Attributed to the advantages, pneumatic rock breaking with CO_2 ice powder has a good application prospect. It is suitable in complex and sensitive construction areas such as adjacent subway or building areas where explosives are prohibited. Furthermore, it can also be used in the field of coal mining for roadway excavation and improving coal seam gas drainage, etc.

6 Conclusions

To improve the efficiency of rock breaking, a site test of the pneumatic rock breaking with CO_2 ice powder was carried out. Considering the effects of vibration induced by rock breaking on surrounding buildings, vibration sensors were installed at different positions and vibration waveforms were collected, so that the dominant frequencies and the PPV at different distances could be obtained. The main conclusions drawn are as follows:

(1) The pneumatic rock breaking with CO_2 ice powder is greatly affected by quasi-static pressure of high-pres-

sure gas. After rock breaking, the macrocracks around the rock breaking boreholes are the main ones without crushing zones, which is different from the rock breaking with explosives. Different breaking boreholes correspond to different directions of cracks, which is mainly related to the direction of principal stress caused by release of high-pressure CO_2 gas.

(2) From the perspective of frequency distribution of waveform, the complexity of pneumatic rock breaking with CO_2 ice powder lies between mechanical rock breaking and explosive blasting. With the increase of distance, the attenuation of high-frequency energy is more severe than that of low-frequency energy. Overall, the dominant frequencies of waveforms close to the rock breaking position are lower. More than 57 m away from the rock breaking point, the dominant frequencies of the vibration waveforms generally do not change.

(3) The PPV induced by the pneumatic rock breaking with CO_2 ice powder with the distance highly conforms to the power function, which is slower than that induced by the hydraulic breaker. For the hydraulic breaker and pneumatic rock breaking with CO_2 ice powder, the PPV attenuates unstably with the distance, which can be divided into three stages, namely the rapid descent region, slow descent region and stable region.

(4) When the vibration propagates downward along the slope, the vibration waves are reflected and refracted on the slope, and the wave impedance increases from top to bottom. For these reasons, the PPV induced by the pneumatic fracturing with CO_2 ice powder attenuates rapidly along the slope. The steeper the slope, the more quickly does the PPV attenuate.

(5) The PPV induced by the pneumatic rock breaking with CO_2 ice powder reduces down to 21.9 mm/s at the distance of 2.8 m, which meets the requirements for vibration velocity threshold of general buildings mentioned in safety standards for blasting vibration. This rock breaking process thus is safer and more reliable than traditional liquid carbon dioxide rock breaking and explosive blasting. It significantly improves the rock breaking efficiency.

References

Ambraseys NR, Hendron AJ (1968) Dynamic behaviour of rock masses rock mechanics in engineering, practices. Wiley, London

Bayat P, Monjezi M, Rezakhah M et al (2020) Artificial neural network and firefly algorithm for estimation and minimization of ground vibration induced by blasting in a mine. Nat Resour Res. https://doi.org/10.1007/s11053-020-09697-1

Carnevale M, Young G, Hager J (2000) Monitoring of TBM-induced ground vibrations. In: Ozdemir L (ed) North American tunneling. Balkema, Rotterdam, pp 374–384

Chen HD, Wang ZF, Qi LL et al (2017) Effect of liquid carbon dioxide phase change fracturing technology on gas drainage. Arab J Geosci 10:314

Chi LY, Zhang ZX, Aalberg A et al (2019) Experimental investigation of blast-induced fractures in rock cylinders. Rock Mech Rock Eng 52:2569–2584

Davies B, Farmer IW, Attewell PB (1964) Ground vibrations from shallow sub-surface blasts. Engineer 217:553–559

Donzé FV, Bouchez J, Magnier SA (1997) Modeling fractures in rock blasting. Int J Rock Mech Min 34(8):1153–1163

Duvall WI, Fogelson DE (1962) Review of criteria for estimating damages to residences from blasting vibrations. R. I. 5968. US, Bureau of Mines, Washington, DC

Feng XJ, Zhang QM, Wang EY et al (2020) 3D modeling of the influence of a splay fault on controlling the propagation of nonlinear stress waves induced by blast loading. Soil Dyn Earthq Eng 138:106335

Gao MS, Dou LM, Zhang N et al (2007) Experimental study on tremor for transmitting law of rockburst in geomaterials. Chin J Rock Mech Eng 26(7):1365–1371

Gao F, Tang L, Zhou K et al (2018a) Mechanism analysis of liquid carbon dioxide phase transition for fracturing rock masses. Energies. https://doi.org/10.3390/en11112909

Gao QD, Lu WB, Yang ZW et al (2018b) Analysis of evolution of seismic components induced by a vertical blasthole. Rock Mech Rock Eng 52:1959–1977

Genet M, Yan WY, Tran-Cong T (2009) Investigation of a hydraulic impact: a technology in rock breaking. Arch Appl Mech 79:825–841

Global J (1995) Cardox system brings benefits in the mining of large coal. Coal Int 243:27–28

Grund M, Ritter J, Gehrig M (2016) Ground motion relations while TBM drilling in unconsolidated sediments. Rock Mech Rock Eng 49(5):1–15

Hajihassani M, Jahed Armaghani D, Marto A et al (2015) Ground vibration prediction in quarry blasting through an artificial neural network optimized by imperialist competitive algorithm. B Eng Geol Environ 74(3):873–886

Hashemi AS, Katsabanis P (2020) The effect of stress wave interaction and delay timing on blast-induced rock damage and fragmentation. Rock Mech Rock Eng 53(5):2327–2346

Hu SB, Pang SG, Yan ZY (2019) A new dynamic fracturing method: deflagration fracturing technology with carbon dioxide. Int J Fracture 220(1):99–111

Huang X, Liu QS, Liu H et al (2018) Development and in-situ application of a real-time monitoring system for the interaction between TBM and surrounding rock. Tunn Undergr Sp Tech 81(2018):187–208

Huang JH, Yi L, Zhang G et al (2020) Numerical analysis on rock blasting damage in Xiluodu underground powerhouse using an improved constitutive model. Eur J Environ Civ En. https://doi.org/10.1080/19648189.2020.1780475

Jahed Armaghani D, Hajihassani M, Mohamad ET et al (2014) Blasting-induced flyrock and ground vibration prediction through an

expert artificial neural network based on particle swarm optimization. Arab J Geosci 7:5383–5396

Jahed Armaghani D, Raja SNSB, Faizi K et al (2015) Developing a hybrid PSO–ANN model for estimating the ultimate bearing capacity of rock-socketed piles. Neural Comput Appl 28(2):391–405

Khandelwal M, Singh TN (2006) Prediction of blast induced ground vibrations and frequency in opencast mine: a neural network approach. J Sound Vib 289(4–5):711–725

Khandelwal M, Singh TN (2007) Evaluation of blast-induced ground vibration predictors. Soil Dyn Earthq Eng 27(2):116–125

Kumar S, Mishra AK (2020) Reduction of blast-induced ground vibration and utilization of explosive energy using low-density explosives for environmentally sensitive areas. Arab J Geosci. https://doi.org/10.1007/s12517-020-05645-8

Li BL, Li N, Wang EY et al (2017a) Characteristics of coal mining microseismic and blasting signals at Qianqiu coal mine. Environ Earth Sci 76(21):722

Li BL, Li N, Wang EY et al (2017b) Discriminant model of coal mining microseismic and blasting signals based on waveform characteristics. Shock Vib 2017:1–13

Li QY, Liu XX, Wu ZY et al (2018) Application of liquid CO2 phase change rock breaking technology in metro foundation pit excavation. J Railw Sci Eng 15(1):163–169

Li QY, Chen G, Luo DY et al (2020) An experimental study of a novel liquid carbon dioxide rock-breaking technology. Int J Rock Mech Min 128(2020):1–9

Liu SJ, Huang ZH (2019) Feasibility study on the application of carbon dioxide phase change fracturing technology in a foundation pit of an open cut tunnel. Vibroengineering PROCEDIA 29(7):295–300

Matidza MI, Zhang JH, Hang G et al (2020) Assessment of blast-induced ground vibration at Jinduicheng molybdenum open pit mine. Nat Resour Res. https://doi.org/10.1007/s11053-020-09623-5

Monjezi M, Hasanipanah M, Khandelwal M et al (2013) Evaluation and prediction of blast-induced ground vibration at Shur River Dam, Iran, by artificial neural network. Neural Comput Appl 22(7–8):1637–1643

Nateghi R, Goshtasbi K, Nejati HR (2020) Prediction of shear strain induced by blasting waves in surface structures based on coupled frequency, velocity, and displacement effects. J Vib Control. https://doi.org/10.1177/1077546320935259

Radojica L, Kostic S, Pantovic R et al (2014) Prediction of blast-produced ground motion in a copper mine. Int J Rock Mech Min 69:19–25

Roy MP, Singh PK, Sarim M et al (2016) Blast design and vibration control at an underground metal mine for the safety of surface structures. Int J Rock Mech Min 83:107–115

Roy MP, Mishra AK, Agrawal H et al (2020) Blast vibration dependence on total explosives weight in open-pit blasting. Arab J Geosci. https://doi.org/10.1007/s12517-020-05560-y

Roy PP (1991) Prediction and control of ground vibrations due to blasting. Colliery Gaurdian 239(7):215–219

Sampath KHSM, Perera MSA, Elsworth D et al (2019) Effect of coal maturity on CO2-based hydraulic fracturing process in coal seam gas reservoirs. Fuel 236:179–189

Singh CP, Agrawal H, Mishra AK (2020) A study on influence of blast-induced ground vibration in dragline bench blasting using signature hole analysis. Arab J Geosci. https://doi.org/10.1007/s12517-020-05562-w

Tang H (2007) Field experimental and theoretical study on blasting wave propagation charcteristics under different terrains. Dissertation of Chinese Academy of Sciences

Wang ZW, Li XB, Peng K et al (2015) Impact of blasting parameters on vibration signal spectrum: determination and statistical evidence. Tunn Undergr Space Technol 48(4):94–100

Xu XF, Dou LM, Lu CP et al (2010) Frequency spectrum analysis on micro-seismic signal of rock bursts induced by dynamic disturbance. Int J Min Sci Technol 20(5):682–685

Yan ZY, Hu SB, Bian Y et al (2019) Experimental study on the mass ratio of dry ice power pneumatic fracturing concrete. Eng Blast 5:14–18

Yang RL, Rocque P, Katsabanis P et al (1994) Measurement and analysis of near-field blast vibration and damage. Geotech Geol Eng 12:169–182

Yang XF, Li YH, Nie AG et al (2020) Numerical study on rock breaking mechanism of supercritical CO_2 jet based on smoothed particle hydrodynamics. Comp Model Eng 122(3):1141–1157

Zhang YN, Deng JR, Deng HW et al (2018) Peridynamics simulation of rock fracturing under liquid carbon dioxide blasting. Int J Damage Mech 28(4):1–15

Zhong QL (2018) Experimental study on millisecond blasting base on slope elevation amplification effect. Jiangxi Univ Sci Technol

Zhou ST, Jiang N, He X et al (2020a) Rock breaking and dynamic response characteristics of carbon dioxide phase transition fracturing considering the gathering energy effect. Energies 13:1–16

Zhou W, Li Z, Wu X et al (2020b) A novel method to evaluate the effect of slope blasting under impact loading. Shock Vib 12:1–17

Publisher's Note Springer Nature remains neutral with regard to jurisdictional claims in published maps and institutional affiliations.